Boron Supercapacitors

Cheng Zhan,[1] Pengfei Zhang,[2] Sheng Dai,[2,3] and De-en Jiang[1,*]

[1]Department of Chemistry, University of California, Riverside, CA 92521, United States

[2]Chemical Sciences Division, Oak Ridge National Laboratory, Oak Ridge, TN 37831-6201, United States

[3]Department of Chemistry, The University of Tennessee, Knoxville, TN 37996-1600, United States

*E-mail: de-en.jiang@ucr.edu. Tel.: +1-951-827-4430

(*ACS Energy Letters; accepted 16 November 2016*)

Abstract: Supercapacitors based on the electric double-layer mechanism use porous carbons or graphene as electrodes. To move beyond this paradigm, we propose boron supercapacitors to leverage 2D boron sheets' metallicity and light weight. Six 2D boron sheets from both previous theoretical design and experimental growth are chosen as test electrodes. By using joint density functional theory (JDFT) to the electrode/electrolyte system, we examine how the 2D boron sheets charge up against applied potential. JDFT predicts that these 2D boron sheets exhibit specific capacitance on the order of 400 F/g, about four times of that of graphene. Our work suggests that 2D boron sheets are promising electrodes for supercapacitor applications.

TOC Figure

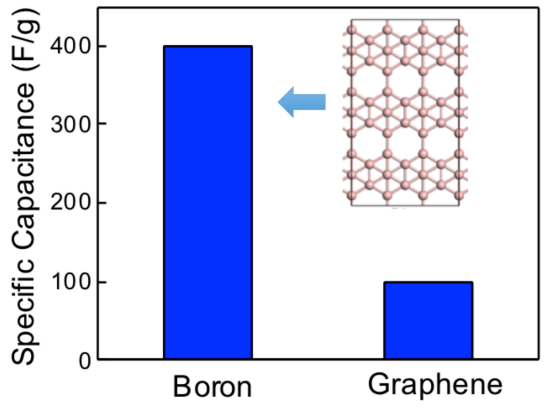

Supercapacitors have much higher power density than batteries and much greater capacities than conventional dielectric or electrolytic capacitors. They store electric energy electrochemically[1-5] and can be divided into two main types: electric double layer capacitors (EDLCs) and pseudocapacitors. EDLCs stores electrical energy by the formation of electric double layers at the electrode/electrolyte interface, while pseudocapacitors store energy via reversible redox reactions at the electrode surface.[6-8] Due to the simple mechanism of electrostatic charge separation and absence of chemical reactions, EDLCs have much longer cycle life than pseudocapacitors.

Activated carbon is the most widely used electrode material for EDLCs because of its low cost, good conductivity, and chemical stability.[9-13] Many other types of porous carbons have also been explored for EDLCs, including carbide-derived carbons[14, 15] and other nanostructured carbons.[16] The specific capacitance of these carbon materials ranges from 100 to 200 F/g.[1] Due to its high specific surface area (~ 2600 m^2/g) and conductivity,[17-20] the specific capacitance of graphene has been measured recently: it is about 130 F/g in aqueous electrolyte and 90 F/g in ionic liquid.[8] Graphene EDLCs also exhibit very long cycle life.[21] However, unlike a traditional metal electrode, the total capacitance of graphene is limited by its quantum capacitance (C_Q), due to its low density of states (DOS) near the Fermi level.[22-25] To address this issue, one promising way is to dope the graphene with heteroatoms such as nitrogen to increase the DOS at the Fermi level (in other words, making it more metallic). This strategy has been explored both experimentally and theoretically in many previous studies.[26-34]

A new idea to move beyond graphene EDLCs in terms of specific capacitance is to use a lighter and more metallic material. This idea leads us to boron. There is a recent surge of interest in exploring novel 2D structures of boron.[35, 36] Theoretical studies suggested many possible types

of structures of boron, including $\boldsymbol{\alpha}$/$\boldsymbol{\beta}$/$\boldsymbol{\gamma}$/**g** types and the less stable triangular and hexagonal sheets.[37-41] The density and configuration of the holes in the 2D hexagonal lattice are important indicators of the relative stability of different types of the 2D boron sheet.[37, 41] Recently, Wu et al. successfully synthesized a stable 2D boron sheet on the Ag(111) surface and visualized the structure by scanning tunneling microscope (STM).[42] The experimentally obtained structures are named $\boldsymbol{\beta}$12 and $\boldsymbol{\chi}$3 whose hole density ($\boldsymbol{\eta}$) is higher than 1/8.[42] The $\boldsymbol{\beta}$12 structure has been theoretically predicted before,[43] while $\boldsymbol{\chi}$3 is a new configuration. Since the 2D boron sheets can have higher specific surface area than graphene and some of them were predicted to be metallic,[43] we believe that 2D boron could be a promising electrode material for supercapacitors. To test this idea, we choose six typical 2D boron configurations and simulate their performance for capacitive energy storage. We show that they are highly promising for EDLC applications.

The six chosen configurations based on previous experimental and theoretical studies are shown in Figure 1. They differ in hole density ($\boldsymbol{\eta}$ values) and the arrangement of the holes. The 2D boron sheets are modeled with the B-B bond length of 1.70 Å, very close to many previous theoretical simulation results.[37, 38] To simulate their charge capacitive behavior, we applied joint density functional theory (JDFT) developed by Arias et al.,[44, 45] which solves the electrode/electrolyte system self-consistently and is implemented in the code JDFTx v.0.99. Periodic boundary condition was applied to describe the interface; the two sides of the 2D boron electrode were solvated by a 10-Å electrolyte described by a polarizable continuum model (PCM) called the charge-asymmetric nonlocally-determined local-electric (CANDLE) solvation model which explicitly takes into account the solvent charge asymmetry.[45] This solvation model improves upon the linear[44] and nonlinear PCM[46] implementations in JDFT. Here we use the CANDLE model to simulate a 6M aqueous solution. The exchange-correlation energy of the

electronic system was calculated by generalized gradient approximation in the form of Perdew-Burke-Ernzerhof functional (GGA-PBE).[47] Ultrasoft pseudopotential was used to describe the nuclei-electron interaction in boron, with 30 Hartree cutoff energy for the plane wave basis.[48] A 24×24×1 k-point mesh was used to sample the Brillouin zone to accurately capture the electron-density optimization at fixed potential calculations in JDFT. To simulate the capacitance, we first fixed the electronic chemical potential on the electrode (ψ) and then computed the surface charge density on the electrode (Q) from the self-consistent JDFT calculation.[49] The differential capacitance of the boron electrode is defined by the derivative of Q vs. ψ: $C_D = dQ/d\psi$, while the integral capacitance is defined as: $C_I = Q/(\psi - \psi_{PZC})$, where ψ_{PZC} is the potential at the point of zero charge. More details of the methodology and the calculations are provided in Supporting Information.

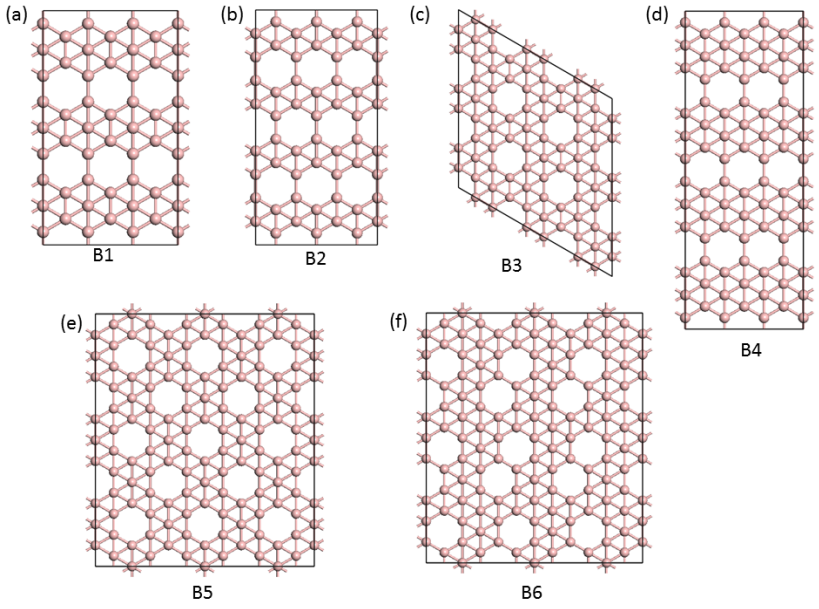

Figure 1. Structure models of the six 2D boron sheets examined in this work: (a) B1, 3×3 supercell; (b) B2, 3×2 supercell; (c) B3, 3×3 supercell; (d) B4, 3×2 supercell; (e) B5, 3×3 supercell; (f) B6, 3×3 supercell.

We first examine the stability and electronic structure of the six typical 2D boron or borophene structures in Figure 1. We calculated their cohesive energy (E_b) according to: $E_b = E_{atom} - E_{sheet}$, where E_{atom} is the energy of a single boron atom in the ^2P state and E_{sheet} is the energy per atom of a 2D boron sheet. So more positive E_b, more stable the structure. From Table 1, one can see that the calculated E_b of the six boron sheets varies from 5.84 to 5.90 eV/atom, consistent with previous DFT results.[37] B3, B4, B5, and B6 have about the same stability (within 0.02 eV/atom) and are about 0.05 eV more stable than B1 and B2 because their lower $\boldsymbol{\eta}$ values are closer to the optimal $(1/9 \text{ and } 2/15)$ as predicted by Ismail-Beigi and Yakobson.[37, 41] Electronic density of states (DOS) in Figure 2 shows that all the six boron sheets are metallic, indicating that they will be good electrode materials for supercapacitors.

Table 1. Hole density ($\boldsymbol{\eta}$), calculated cohesive energy (E_b), and potential at the point of zero charge (PZC) of the six boron sheets

Model[a]	$\boldsymbol{\eta}$	E_b (eV/atom)	ψ_{PZC} vs. SHE (V)
B1 ($\boldsymbol{\beta}12$)	1/6	5.85	0.06
B2 ($\boldsymbol{\chi}3$)	1/5	5.84	-0.04
B3 (new $\boldsymbol{\alpha}$)	1/9	5.90	-0.69
B4 (new $\boldsymbol{\beta}$)	1/7	5.88	-0.39
B5 ($\boldsymbol{\alpha}1$)	1/8	5.90	-0.55
B6 ($\boldsymbol{\beta}1$)	1/8	5.88	-0.46
Graphene	-	-	-0.58

[a]The notations in the parentheses are from the literature: $\boldsymbol{\beta}12$ and $\boldsymbol{\chi}3$ from ref. [42]; new $\boldsymbol{\alpha}$ and new $\boldsymbol{\beta}$ from ref. [37]; $\boldsymbol{\alpha}1$ and $\boldsymbol{\beta}1$ from ref.[43].

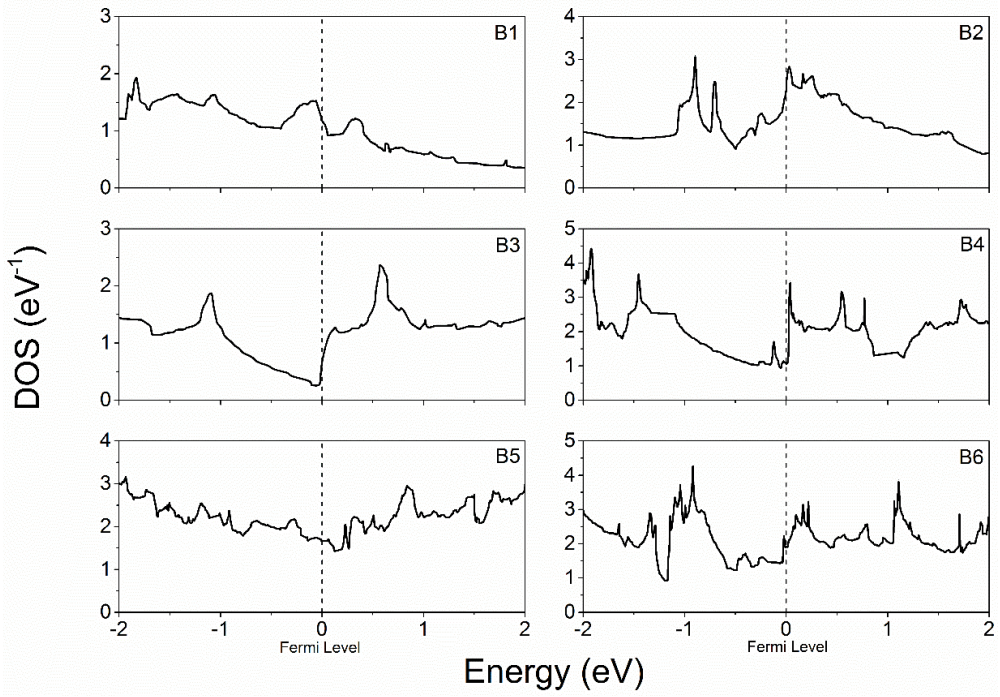

Figure 2. Total electronic density of states (DOS) of the six boron sheets as labeled in Figure 1.

Potential at the point of zero charge (ψ_{PZC}) is an important quantity of an electrode that one can use to evaluate the electrochemical window of charging for an electrode/electrolyte interface. The calculated ψ_{PZC} values of the six 2D boron sheets from JDFT referenced to the standard hydrogen electrode (SHE) are listed in Table 1. One can see that the predicted PZC values of B3 to B6 are quite close to that of graphene, implying that the voltage windows of commonly used electrolytes such as KOH for graphene electrodes will also be suitable for charging the 2D boron electrodes. Although the ψ_{PZC} values of B1 and B2 are higher, the difference (~ 0.6 V) is much less than the voltage windows of common electrolytes (~ 1.2 V for aqueous and ~ 2.5 V for organic electrolytes).

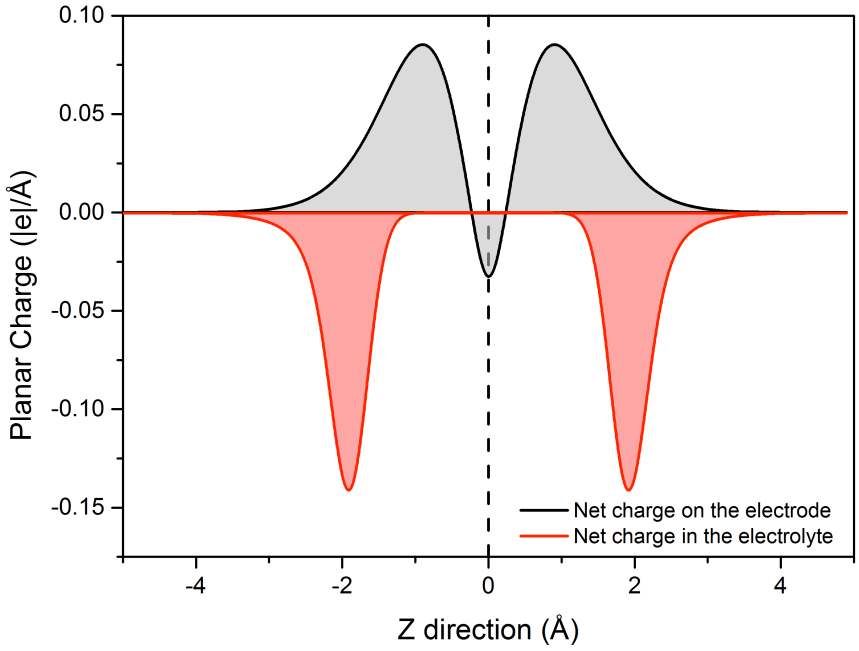

Figure 3. The net charge distribution of the electrode/electrolyte system along the z direction, where the position of the B1 sheet is at z=0 Å; the electrode bias potential is 1 V vs. PZC

We next examined how the 2D boron sheets respond to negative and positive charging up to 1 V relative to the ψ_{PZC}. Figure 3 shows a typical charging state of the electrode/electrolyte interface in the JDFT calculation, where the electrode is at 1 V vs. PZC. One can see that the positive charge on the electrode centers at above 1 Å away the plane of the boron nuclei, while the electrolyte ions (or the Helmholtz layer) peaks at 2 Å away from the boron plane. By integrating the planar charge on the electrode, we can obtain the surface charge density, Q. Figure 4 shows how the surface charge density (Q) changes with the applied potential (ψ). One can see that all of the 2D boron sheets examined can store more charge than graphene at the same applied potential.

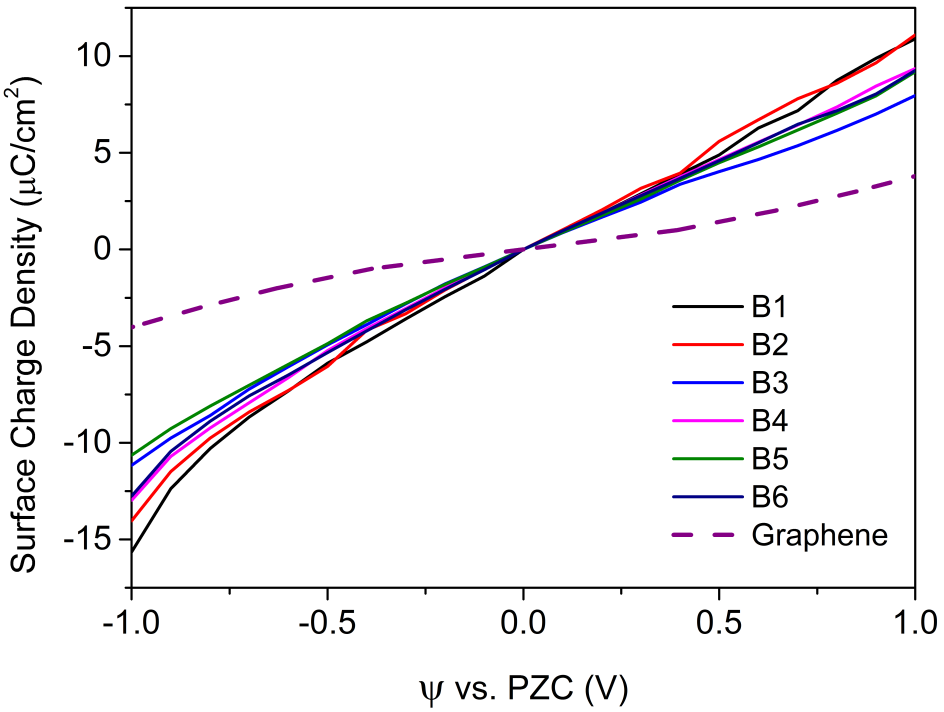

Figure 4. Surface charge density (Q) vs. applied potential (ψ) curves of the six 2D boron sheets, in comparison with that of graphene.

By differentiating the numerically fitted Q vs. ψ curves, we obtained the area-normalized differential capacitance in Figure 5. One can see that the differential capacitance of graphene is about 3 to 5 μF/cm^2, much lower than those of the 2D boron sheets. The differential capacitances of B1 and B2 boron sheets are highest, ranging from 20-30 μF/cm^2 at the -1 V to 13-15 μF/cm^2 at the 1 V and never lower than 12 μF/cm^2. The charging asymmetry or the higher capacitance at the negative voltages is related to the asymmetric response of the boron sheets' electronic structure to the applied potential across the electrode/electrolyte interface. The asymmetric electrolyte response in aqueous electrolyte has been experimentally observed at metal electrode surface.[50] The asymmetry can arise from either the EDL capacitance (for example, the solvation model) or the quantum capacitance. We compared the CANDLE model with the linear PCM

model (Figure S1) and found that indeed the CANDLE model gives more charge response at the negative side, while the linear PCM model gives more symmetric charging. This difference confirms the effect of explicitly treating solvent charge asymmetry in the CANDLE model. In addition, we separately computed quantum capacitance of B1-B6 through the fixed-band-approximation (Figure S2),[22] and found that they all show non-symmetric behavior. Hence, quantum capacitance also contributes to the asymmetric charging as seen in Figure 5.

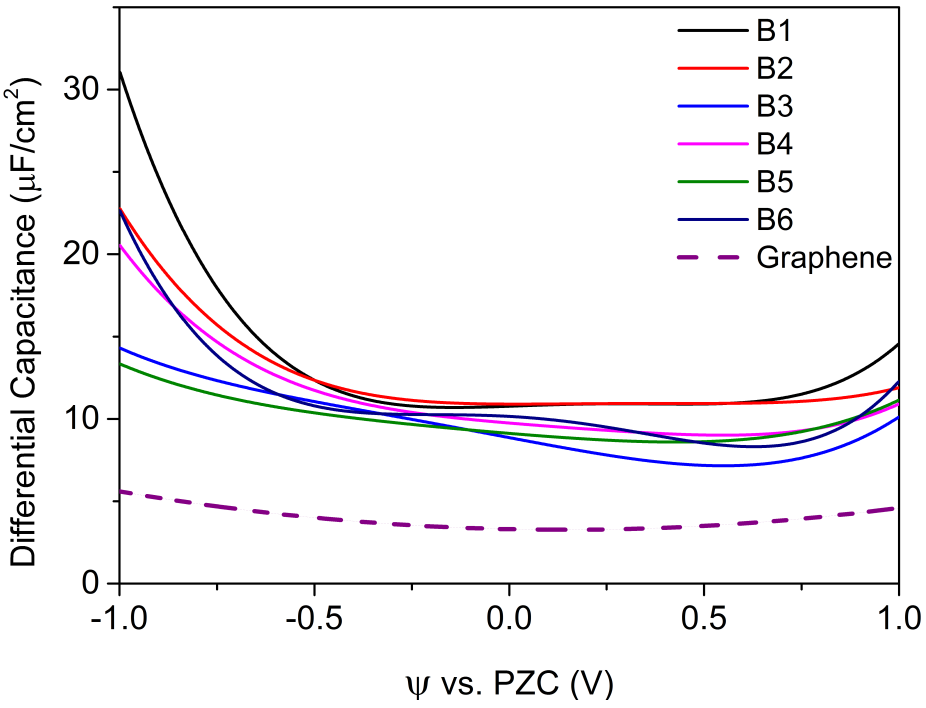

Figure 5. Differential capacitance of 2D boron sheets (obtained from differentiation on the numerically fitted Q- ψ curves in Figure 4).

Specific or gravimetric capacitance is an important measure to compare the performances of different electrode materials for EDLCs. We calculated the integral specific capacitance of the six 2D boron sheets for the voltage window from -0.6 V to 0.6 V around ψ_{PZC} in Figure 6,

corresponding to charging in an aqueous electrolyte. For comparison, the calculated specific capacitance of graphene is 92.6 F/g in the same voltage window. 2D boron sheets show much higher capacitances, partly due to their light weight. The B1 and B2 structures possess very large specific capacitance close to 400 F/g, nearly four times of that of graphene. The other four structures (B3 to B6) have specific capacitance around 300 F/g. Thus, our results show that 2D boron sheets are a very promising electrode material for EDLCs.

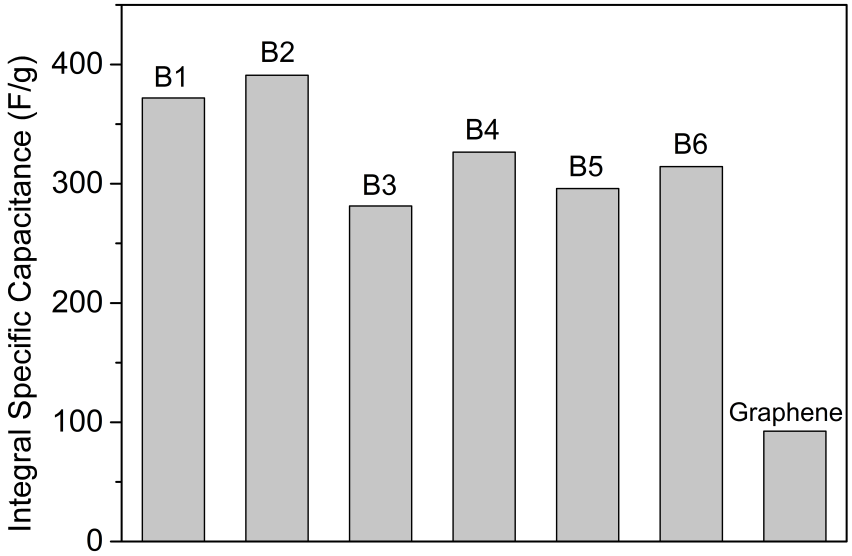

Figure 6. Calculated Integral specific capacitance of 2D boron sheets in the voltage window of -0.6 V to 0.6 V around ψ_{PZC}.

Comparison between our predicted capacitance and the experimental measurements for graphene can offer an estimate of the accuracy for our predicted capacitances for the 2D boron sheets. In 2008, Rouff et al. measured the capacitance of reduced graphene oxide in the KOH electrolyte and obtained a capacitance 100 F/g based on cyclic voltammogram and 135 F/g based on galvanostatic discharge.[8] In 2014, Ruoff et al. measured the areal capacitance of a CVD

graphene sheet with one side in contact with 6M KOH, and obtained an average value of about 6 μF/cm^2, which corresponds to a gravimetric capacitance of 158 F/g based on the specific surface area of graphene at 2630 m^2/g.[17] So our theoretical capacitance of 93 F/g for graphene underestimates the experimental values. Hence our predicted capacitances for the 2D boron sheets are likely to be a conservative estimate.

Given our prediction of the high capacitance of 2D boron EDLCs, we suggest that an electrochemical measurement be done on them. Recent progress in growing 2D boron on a metal substrate[42] leads us to believe that experimental setups similar to capacitance measurement of graphene[25] can translated to 2D boron sheets, for example, impedance measurement to obtain the differential capacitance under a specified bias potential.[51] Although the synthesis of free-standing 2D boron has not been realized yet, several potential alternatives are suggested here: i) Preparing 2D boron by selectively etching the metal substrate; ii) Designing porous boron with thin boron wall while some sacrificial templates may be needed for porosity control; iii) CVD growth of 2D boron-graphene hybrids with high boron loading. Since the technologies for graphene processing are rich, it may be possible to prepare the hybrid for EDLC study. Due to its electron deficiency, the 2D boron sheet could be instable in an aqueous electrolyte, especially during electrochemical charging. This problem can be mitigated by using a non-aqueous electrolyte such as organic electrolytes or ionic liquids which have higher electrochemical windows and less chemical reactivity toward boron. Although we modeled the capacitive performance of 2D boron sheets in an implicit aqueous electrolyte, our conclusion can be equally applied to non-aqueous electrolytes.

In summary, we studied the capacitive performance of 2D boron sheets and found that they exhibit extremely high specific capacitance, about three to four times of that of graphene,

due to their metallicity and light weight. Hence we suggest boron as a very promising EDLC electrode. The huge potential of 2D boron sheets in supercapacitor applications as computationally demonstrated here invites experiments to examine their electrochemical behavior, and the recent success in growing single-layer boron sheets laid foundation for such efforts.

Supporting Information

The Supporting Information is available free of charge on the ACS Publications website.

- Method details
- Comparison of linear PCM and CANDLE solvation models.
- Contribution of quantum capacitance.

Acknowledgement

This research is sponsored by the Fluid Interface Reactions, Structures, and Transport (FIRST) Center, an Energy Frontier Research Center funded by the U.S. Department of Energy (DOE), Office of Science, Office of Basic Energy Sciences. This research used resources of the National Energy Research Scientific Computing Center, a DOE Office of Science User Facility supported by the Office of Science of the U.S. Department of Energy under Contract No. DE-AC02-05CH11231.

References:

(1) Zhang, L. L.; Zhao, X. S. Carbon-Based Materials as Supercapacitor Electrodes. *Chem. Soc. Rev.* **2009**, *38*, 2520-2531.

(2) Wang, J.; Polleux, J.; Lim, J.; Dunn, B. Pseudocapacitive Contributions to Electrochemical Energy Storage in TiO_2 (Anatase) Nanoparticles. *J. Phys. Chem. C* **2007**, *111*, 14925-14931.

(3) Sassin, M. B.; Chervin, C. N.; Rolison, D. R.; Long, J. W. Redox Deposition of Nanoscale Metal Oxides on Carbon for Next-Generation Electrochemical Capacitors. *Acc. Chem. Res.* **2013**, *46*, 1062-1074.

(4) Sarangapani, S.; Tilak, B. V.; Chen, C. P. Materials for Electrochemical Capacitors - Theoretical and Experimental constraints. *J. Electrochem. Soc.* **1996**, *143*, 3791-3799.

(5) Makino, S.; Ban, T.; Sugimoto, W. Towards Implantable Bio-Supercapacitors: Pseudocapacitance of Ruthenium Oxide Nanoparticles and Nanosheets in Acids, Buffered Solutions, and Bioelectrolytes. *J. Electrochem. Soc.* **2015**, *162*, A5001-A5006.

(6) Zhai, Y. P.; Dou, Y. Q.; Zhao, D. Y.; Fulvio, P. F.; Mayes, R. T.; Dai, S. Carbon Materials for Chemical Capacitive Energy Storage. *Adv. Mater.* **2011**, *23*, 4828-4850.

(7) Wang, Y.; Shi, Z. Q.; Huang, Y.; Ma, Y. F.; Wang, C. Y.; Chen, M. M.; Chen, Y. S. Supercapacitor Devices Based on Graphene Materials. *J. Phys. Chem. C* **2009**, *113*, 13103-13107.

(8) Stoller, M. D.; Park, S. J.; Zhu, Y. W.; An, J. H.; Ruoff, R. S. Graphene-Based Ultracapacitors. *Nano Lett.* **2008**, *8*, 3498-3502.

(9) Yang, X. W.; Cheng, C.; Wang, Y. F.; Qiu, L.; Li, D. Liquid-Mediated Dense Integration of Graphene Materials for Compact Capacitive Energy Storage. *Science* **2013**, *341*, 534-537.

(10) Wang, Y. F.; Yang, X. W.; Qiu, L.; Li, D. Revisiting the Capacitance of Polyaniline by Using Graphene Hydrogel Films as a Substrate: the Importance of Nano-architecturing. *Energ Environ. Sci.* **2013**, *6*, 477-481.

(11) Hahm, M. G.; Reddy, A. L. M.; Cole, D. P.; Rivera, M.; Vento, J. A.; Nam, J.; Jung, H. Y.; Kim, Y. L.; Narayanan, N. T.; Hashim, D. P., et al. Carbon Nanotube-Nanocup Hybrid Structures for High Power Supercapacitor Applications. *Nano Lett.* **2012**, *12*, 5616-5621.

(12) Futaba, D. N.; Hata, K.; Yamada, T.; Hiraoka, T.; Hayamizu, Y.; Kakudate, Y.; Tanaike, O.; Hatori, H.; Yumura, M.; Iijima, S. Shape-Engineerable and Highly Densely Packed Single-Walled Carbon Nanotubes and Their Application as Super-capacitor Electrodes. *Nat. Mater.* **2006**, *5*, 987-994.

(13) Huang, P.; Lethien, C.; Pinaud, S.; Brousse, K.; Laloo, R.; Turq, V.; Respaud, M.; Demortiere, A.; Daffos, B.; Taberna, P. L., et al. On-Chip and Freestanding Elastic Carbon Films for Micro-Supercapacitors. *Science* **2016**, *351*, 691-695.

(14) Chmiola, J.; Largeot, C.; Taberna, P. L.; Simon, P.; Gogotsi, Y. Monolithic Carbide-Derived Carbon Films for Micro-Supercapacitors. *Science* **2010**, *328*, 480-483.

(15) Gogotsi, Y.; Nikitin, A.; Ye, H. H.; Zhou, W.; Fischer, J. E.; Yi, B.; Foley, H. C.; Barsoum, M. W. Nanoporous Carbide-Derived Carbon with Tunable Pore Size. *Nat. Mater.* **2003**, *2*, 591-594.

(16) Candelaria, S. L.; Shao, Y. Y.; Zhou, W.; Li, X. L.; Xiao, J.; Zhang, J. G.; Wang, Y.; Liu, J.; Li, J. H.; Cao, G. Z. Nanostructured Carbon for Energy Storage and Conversion. *Nano Energy* **2012**, *1*, 195-220.

(17) Ji, H.; Zhao, X.; Qiao, Z.; Jung, J.; Zhu, Y.; Lu, Y.; Zhang, L. L.; MacDonald, A. H.; Ruoff, R. S. Capacitance of Carbon-Based Electrical Double-Layer Capacitors. *Nat. Commun.* **2014**, *5*, 3317.

(18) Uesugi, E.; Goto, H.; Eguchi, R.; Fujiwara, A.; Kubozono, Y. Electric Double-Layer Capacitance between an Ionic Liquid and Few-Layer Graphene. *Sci. Rep.* **2013**, *3*, 1595.

(19) Stoller, M. D.; Magnuson, C. W.; Zhu, Y. W.; Murali, S.; Suk, J. W.; Piner, R.; Ruoff, R. S. Interfacial Capacitance of Single Layer Graphene. *Energ Environ. Sci.* **2011**, *4*, 4685-4689.

(20) Liu, C. G.; Yu, Z. N.; Neff, D.; Zhamu, A.; Jang, B. Z. Graphene-Based Supercapacitor with an Ultrahigh Energy Density. *Nano Lett.* **2010**, *10*, 4863-4868.

(21) Cheng, Y. W.; Lu, S. T.; Zhang, H. B.; Varanasi, C. V.; Liu, J. Synergistic Effects from Graphene and Carbon Nanotubes Enable Flexible and Robust Electrodes for High-Performance Supercapacitors. *Nano Lett.* **2012**, *12*, 4206-4211.

(22) Zhan, C.; Neal, J.; Wu, J.; Jiang, D. E. Quantum Effects on the Capacitance of Graphene-Based Electrodes. *J. Phys. Chem. C* **2015**, *119*, 22297–22303.

(23) Brooksby, P.; Farquhar, A.; Dykstra, H.; Waterland, M.; Downard, A. Quantum Capacitance of Aryldiazonium Modified Large Area Few-Layer Graphene Electrodes. *J. Phys. Chem. C* **2015**, *119*, 25778–25785.

(24) Paek, E.; Pak, A. J.; Hwang, G. S. A Computational Study of the Interfacial Structure and Capacitance of Graphene in [BMIM][PF_6] Ionic Liquid. *J. Electrochem. Soc.* **2013**, *160*, A1-A10.

(25) Xia, J. L.; Chen, F.; Li, J. H.; Tao, N. J. Measurement of the Quantum Capacitance of Graphene. *Nat. Nanotechnol.* **2009**, *4*, 505-509.

(26) Vatamanu, J.; Ni, X. J.; Liu, F.; Bedrov, D. Tailoring Graphene-based Electrodes from Semiconducting to Metallic to Increase the Energy Density in Supercapacitors. *Nanotechnology* **2015**, *26*, 464001.

(27) Wood, B. C.; Ogitsu, T.; Otani, M.; Biener, J. First-Principles-Inspired Design Strategies for Graphene-Based Supercapacitor Electrodes. *J. Phys. Chem. C* **2014**, *118*, 4-15.

(28) Paek, E.; Pak, A. J.; Kweon, K. E.; Hwang, G. S. On the Origin of the Enhanced Supercapacitor Performance of Nitrogen-Doped Graphene. *J. Phys. Chem. C* **2013**, *117*, 5610-5616.

(29) Zhang, L. L.; Zhao, X.; Ji, H. X.; Stoller, M. D.; Lai, L. F.; Murali, S.; Mcdonnell, S.; Cleveger, B.; Wallace, R. M.; Ruoff, R. S. Nitrogen Doping of Graphene and its Effect on Quantum Capacitance, and a New Insight on the Enhanced Capacitance of N-doped Carbon. *Energ Environ. Sci.* **2012**, *5*, 9618-9625.

(30) Zou, Y. Q.; Kinloch, I. A.; Dryfe, R. A. W. Nitrogen-Doped and Crumpled Graphene Sheets with Improved Supercapacitance. *J. Mater. Chem. A* **2014**, *2*, 19495-19499.

(31) Wang, K.; Li, L. W.; Zhang, T. Z.; Liu, Z. F. Nitrogen-Doped Graphene for Supercapacitor with Long-term Electrochemical Stability. *Energy* **2014**, *70*, 612-617.

(32) Wen, Z. H.; Wang, X. C.; Mao, S.; Bo, Z.; Kim, H.; Cui, S. M.; Lu, G. H.; Feng, X. L.; Chen, J. H. Crumpled Nitrogen-Doped Graphene Nanosheets with Ultrahigh Pore Volume for High-Performance Supercapacitor. *Adv. Mater.* **2012**, *24*, 5610-5616.

(33) Zhao, L. Y.; He, R.; Rim, K. T.; Schiros, T.; Kim, K. S.; Zhou, H.; Gutierrez, C.; Chockalingam, S. P.; Arguello, C. J.; Palova, L., et al. Visualizing Individual Nitrogen Dopants in Monolayer Graphene. *Science* **2011**, *333*, 999-1003.

(34) Zhang, C. H.; Fu, L.; Liu, N.; Liu, M. H.; Wang, Y. Y.; Liu, Z. F. Synthesis of Nitrogen-Doped Graphene Using Embedded Carbon and Nitrogen Sources. *Adv. Mater.* **2011**, *23*, 1020-1024.

(35) Boustani, I. New Quasi-Planar Surfaces of Bare Boron. *Surf. Sci* **1997**, *370*, 355-363.

(36) Tai, G. A.; Hu, T. S.; Zhou, Y. G.; Wang, X. F.; Kong, J. Z.; Zeng, T.; You, Y. C.; Wang, Q. Synthesis of Atomically Thin Boron Films on Copper Foils. *Angew Chem Int Edit* **2015**, *54*, 15473-15477.

(37) Tang, H.; Ismail-Beigi, S. Novel Precursors for Boron Nanotubes: The Competition of Two-Center and Three-Center Bonding in Boron Sheets. *Phys. Rev. Lett.* **2007**, *99*, 115501.

(38) Tang, H.; Ismail-Beigi, S. First-Principles Study of Boron Sheets and Nanotubes. *Phys. Rev. B* **2010**, *82*, 115412.

(39) Miller, J. New Sheet Structures may be the Basis for Boron Nanotubes. *Phys. Today* **2007**, *60*, 20-21.

(40) Ozdogan, C.; Mukhopadhyay, S.; Hayami, W.; Guvenc, Z. B.; Pandey, R.; Boustani, I. The Unusually Stable B-100 Fullerene, Structural Transitions in Boron Nanostructures, and a Comparative Study of alpha- and gamma-Boron and Sheets. *J. Phys. Chem. C* **2010**, *114*, 4362-4375.

(41) Penev, E. S.; Bhowmick, S.; Sadrzadeh, A.; Yakobson, B. I. Polymorphism of Two-Dimensional Boron. *Nano Lett.* **2012**, *12*, 2441-2445.

(42) Feng, B. J.; Zhang, J.; Zhong, Q.; Li, W. B.; Li, S.; Li, H.; Cheng, P.; Meng, S.; Chen, L.; Wu, K. H. Experimental Realization of Two-Dimensional Boron Sheets. *Nat. Chem.* **2016**, *8*, 564-569.

(43) Wu, X. J.; Dai, J.; Zhao, Y.; Zhuo, Z. W.; Yang, J. L.; Zeng, X. C. Two-Dimensional Boron Monolayer Sheets. *Acs Nano* **2012**, *6*, 7443-7453.

(44) Letchworth-Weaver, K.; Arias, T. A. Joint Density Functional Theory of the Electrode-Electrolyte Interface: Application to Fixed Electrode Potentials, Interfacial Capacitances, and Potentials of Zero Charge. *Phys. Rev. B* **2012**, *86*, 075140.

(45) Sundararaman, R.; Goddard, W. A. The Charge-Asymmetric Nonlocally Determined Local-Electric (CANDLE) Solvation Model. *J. Chem. Phys.* **2015**, *142*, 064107.

(46) Gunceler, D.; Letchworth-Weaver, K.; Sundararaman, R.; Schwarz, K. A.; Arias, T. A. The Importance of Nonlinear Fluid Response in Joint Density-Functional Theory Studies of Battery Systems. *Modell. Simul. Mater. Sci. Eng.* **2013**, *21*, 074005.

(47) Perdew, J. P.; Burke, K.; Ernzerhof, M. Generalized Gradient Approximation Made Simple. *Phys. Rev. Lett.* **1996**, *77*, 3865-3868.

(48) Garrity, K. F.; Bennett, J. W.; Rabe, K. M.; Vanderbilt, D. Pseudopotentials for High-Throughput DFT Calculations. *Comput. Mater. Sci.* **2014**, *81*, 446-452.

(49) Zhan, C.; Jiang, D. Contribution of Dielectric Screening to the Total Capacitance of Few-Layer Graphene Electrodes. *J. Phys. Chem. Lett* **2016**, *7*, 789.

(50) Rosen, M.; Flinn, D. R.; Schuldin.S Double Layer Capacitance on Platinum in 1m H2s04 from Reversible Hydrogen Potential to Oxygen Formation Region. *J. Electrochem. Soc.* **1969**, *116*, 1112.

(51) Segalini, J.; Daffos, B.; Taberna, P. L.; Gogotsi, Y.; Simon, P. Qualitative Electrochemical Impedance Spectroscopy Study of Ion Transport into Sub-nanometer Carbon Pores in Electrochemical Double Layer Capacitor Electrodes. *Electrochim. Acta* **2010**, *55*, 7489-7494.